Electronic Supplementary Information

Suppression of dendritic lithium-metal growth through concentrated dual-salt electrolyte and its accurate prediction

Tai Thai Vu, [a] Byung Gon Kim,*[b] Jung Ho Kim *[c] and Janghyuk Moon*[a]

[a.] *School of Energy Systems Engineering, Chung-Ang University, Heukseok-Ro, Dongjak-Gu, Seoul 06974, Republic of Korea*

[b.] *Next Generation Battery Research Center, Korea Electrotechnology Research Institute (KERI), 12, Jeongiui-gil, Seongsan-gu, Changwon-si, Gyeongsangnam-do 51543, Republic of Korea.*

[c.] *Institute for Superconducting & Electronic Materials (ISEM), Australian Institute of Innovative Materials (AIIM), University of Wollongong, Innovation Campus, Squires Way, North Wollongong, NSW 2500, Australia*

*Corresponding authors: B. G. Kim (byunggonkim@keri.re.kr); J. H. Kim (jhk@uow.edu.au);

J. Moon (jhmoon84@cau.ac.kr)

Experimental methods

Materials

LiFSI (> 98%, TCI, Japan), LiTFSI (99.95%, Sigma-Aldrich, USA), LiNO3 (99.999%, Acros, Belgium), anhydrous DME (99.5%, Sigma-Aldrich, USA), and anhydrous DOL (99.8%, Sigma-Aldrich, USA) were purchased for this study. The LiFSI, LiTFSI, and $LiNO_3$ were vacuum dried at 80 °C prior to their usage. No further purification of the solvents was conducted. An Ar-filled glove box (KOREA KIYON, Korea) was used to prepared the electrolytes. Polyethylene (PE) separator (Celgard 2730, Celgard, USA), and Li metal (20 μm, Honjo, Japan), Cu (18 μm, Hohsen, Japan), and Al (12 μm, Hohsen, Japan) foil were purchased for the cell assembly. Carbon-coated Li–iron–phosphate was provided by Hanwha Chemical Co. (Korea). Finally, 2032 coin-type cell kits were purchased from Hohsen (Japan).

Electrochemical Tests

For the Li-Li symmetric cell testing, the PE separator was sandwiched between 20 μm discs of Li metal foil with three different electrolytes to analyze the morphological changes by *in*-situ OM. For the Li plating tests using SEM, Li-Cu asymmetric cells were assembled by employing Li metal foil (200 μm in thickness) for the reference/counter electrode, PE separator, and Cu foil as the working electrode. A fixed amount of Li was plated on the Cu foil. For the Li-metal full-cell tests, the LFP electrodes were prepared by casting a slurry consisting of 80 % active material, 10 % Super-P (TIMCAL, Switzerland), and 10 % poly(vinylidene difluoride) (PVDF, Aldrich, USA) dispersed in N-methy1-2-pyrrolidone (NMP, Sigma-Aldrich, USA). The well-mixed slurry was cast onto an Al current collector and vacuum-dried at 80 °C for 12 h. The loading level of the LFP electrode was fixed at 14 mg cm^{-2}. Coin-type cells were assembled with 20 μm thick Li-metal foil as a counter electrode in an argon atmosphere. Considering the cathode capacity of 2 mAh cm^{-2}, the negative-to-positive capacity (n/p) ratio was ~2 in this full cell condition. The electrochemical tests were performed at 25 °C using a battery cycler (WBCS3000Le, WonAtech, Korea). Ionic conductivities of each electrolyte were measured using two stainless-steel blocking electrodes via EIS and calculated using the following equation, $\sigma = t/R_bS$, where t is the sample thickness, R_b is the bulk resistance area, and S is the effective contact. A conductivity meter (S30 SevenEasy, Mettler Toledo, Switzerland) was also employed to measure the ionic conductivity.

Characterizations

After the electrochemical tests, the cells were dismantled in an Ar atmosphere and the cycled Li metal electrodes were washed with DME and then vacuum dried in an antechamber, connected directly to the glovebox. The electrode morphologies were analyzed and characterized by field-emission SEM (FE-SEM, S-4800, Hitachi, Japan). *In*-situ OM measurements (BX53M, Olympus, Japan) were conducted in all three optical electrode cells (ECC-Opto-Std, EL-CELL, Germany). For microscopic characterizations, moisture and air contamination were avoided by using an airtight sample box during sample transfer. Depth profiling (Ar^+ cluster ion source, 40° incident angle with 10 keV Ar^+_{1000}) and XPS measurements of the SEI layers were conducted using glovebox-connected XPS (Axis-Supra, Kratos, Japan) using monochromatic Al K_α (1486.6 eV) as the X-ray source. For this test, the SEI layers on the Cu foils in the Li–Cu cells were obtained after 30 cycles at 0.5 mA cm^{-2} and 0.5 mA h cm^{-2}. The C 1s peak at 284.8 eV was used as a reference.

Computational Method

Li deposition and growth behavior was simulated in a two-dimensional pseudo model with symmetric Li cell configurations by moving boundary techniques implemented in COMSOL Multiphysics (Version 5.5) FEM software. Three main governing equations describe the mass movement of the charged species and the distribution of the electric and electrolyte potential. According to Ohm's law, the current density vector *i* that flows through a cross-sectional area centered at a given location is proportional to the electric field, as follows:

$$i = \sigma E \tag{1}$$

where σ is the material-dependent conductivity and E is the electric field at the given location. By considering the electric field in terms of the local gradient of the electric potential $\emptyset$, the behavior of the electric charge current in the electrode domain can be expressed as:

$$i_s = -\sigma_s \nabla \emptyset_s \tag{2}$$

where the subscript *s* indicates that this relationship is applicable to the solid electrode region, σ_s is the electrical conductivity, and ϕ_s is the electric potential of the solid electrode. The charge transfer behavior of the liquid electrolyte region can also be described following Ohm's law as:

$$i_l = \left(- \sigma_l \nabla \emptyset_l \right) + \frac{2\sigma_l RT}{F}\left(1 + \frac{\partial lnf}{\partial lnc_l}\right)(1 - t_+)\nabla lnc_l \tag{3}$$

where the subscript *l* indicates that this relationship is applicable to the liquid electrolyte region, σ_l is the electrolyte ionic conductivity, ϕ_l is the potential of the electrolyte, c_l is the concentration of the electrolyte salt, *T* is the temperature of the cell, *R* is the molar gas constant, and *F* is Faraday's constant. Applying the concentrated solution theory and the Gibbs–Duhem relationship, the flux density of the cations and anions can be respectively expressed as:

$$N_+ = - v_+ D\nabla c + \frac{it_+^0}{z_+ F} \tag{4}$$

$$N_- = - v_- D\nabla c + \frac{it_-^0}{z_- F} \tag{5}$$

where *D* is the diffusivity coefficient of the electrolyte and *t* is the transference number, which is set at 0.36. The mass transport of Li ions in the liquid electrolyte region follows Fisk's second law of diffusion:

$$\frac{\partial_{c_l}}{\partial t} = \nabla.(D_l \nabla c_l) - \frac{i_l t_+}{F} \tag{6}$$

In addition, the interfacial electrochemical kinetics are assumed to follow the concentration-dependent Butler–Volmer relationship. The charge transport behavior on the electrode–electrolyte interface is then described as:

$$i = i_0\left(C_R \exp\left(\frac{(1-\alpha)F}{RT}\eta\right) - C_O exp\left(\frac{\alpha F}{RT}\eta\right)\right) \tag{7}$$

where *i* is the local current density on the electrolyte–electrode surface; i_0 is the reference exchange current density; C_R and C_O are the time–dependent concentrations of the reduced and oxidized species, respectively; α is the charge transfer coefficient, which is set at 0.5; and η is the activation overpotential of the redox reaction. The Li growth velocity on the electrode–electrolyte interface boundary is defined by its linear relationship with the local current density:

$$v = \frac{iM}{F\rho} \tag{8}$$

where *M* and ρ are the molecular weight and the volumetric mass density of Li, respectively. At every simulation time step, the Li metal geometry is updated by calculating the deposition volume of the Li metal and then re-meshed when it does not match. The values used in this work are shown in Table S1.

Because most components of the SEI have low ionic conductivities near 10^{-6} S cm^{-1} (Table S2), the values of Li^+ ionic conductivities were used 1.1×10^{-6} S cm^{-1} for both 1LTF and 2LF electrolytes. However, LN electrolyte generate a plentiful of Li_3N components in SEI layer. We set to be 1.0×10^{-6} S cm^{-1} of the Li^+ ionic conductivities in LN electrolytes. This value can represent the value of most SEI components which show fast ionic conductivities in the range from 10^{-3} to 10^{-4} S cm^{-1}. Symmetric Li cell models with various nucleation seeds and operating conditions were employed to analyze the role of the electrolyte concentration and ionic conductivity of the SEI/electrolyte in regulating Li dendrite growth in the LMB.

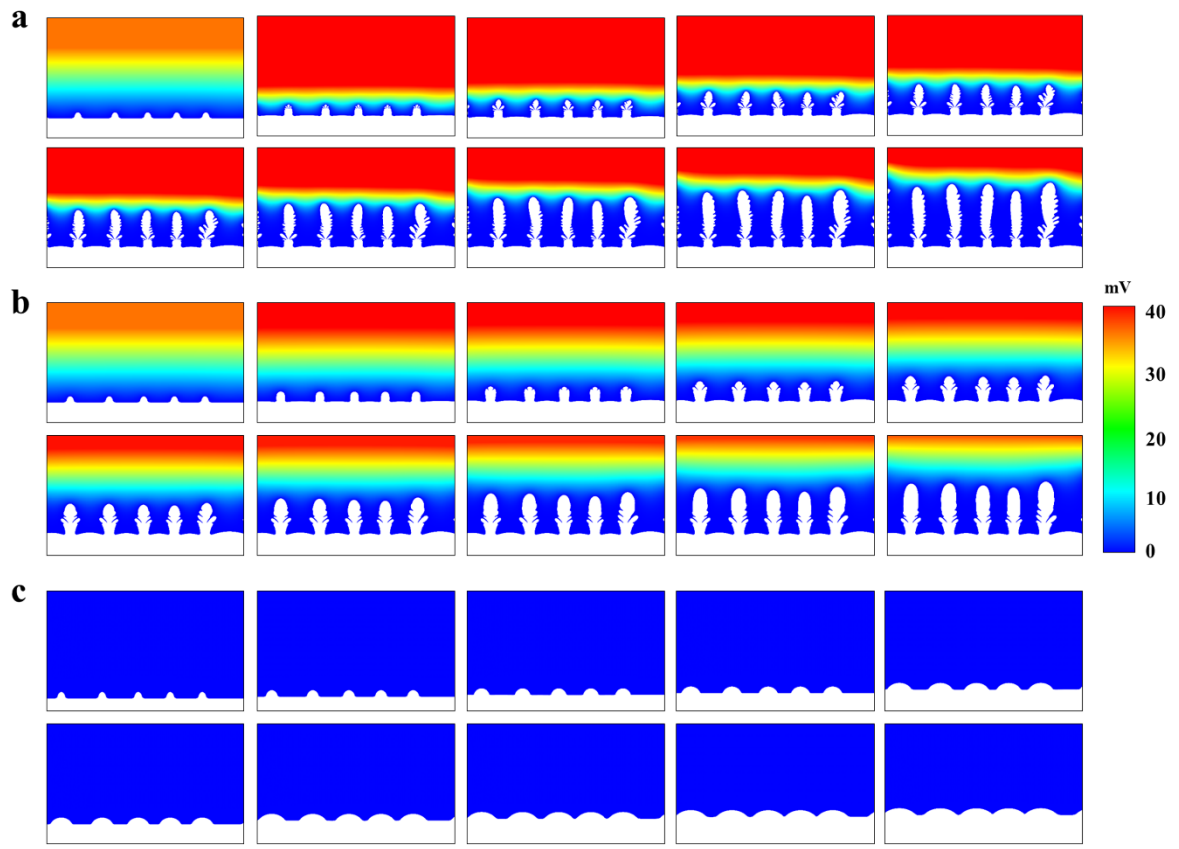

Fig. S1 Evolution of the potential profile of the (a) 1 M LiTFSI in DOL/DME with 1% LiNO3 (1LTF), (b) 4 M LiFSI in DME (4LF), and (c) 2 M LiFSI and 2 M LiNO3 in DME (2LN2LF) electrolyte systems at 0.25 mA cm−2 in 1000 s. The snapshots are obtained at a time step of 100 s.

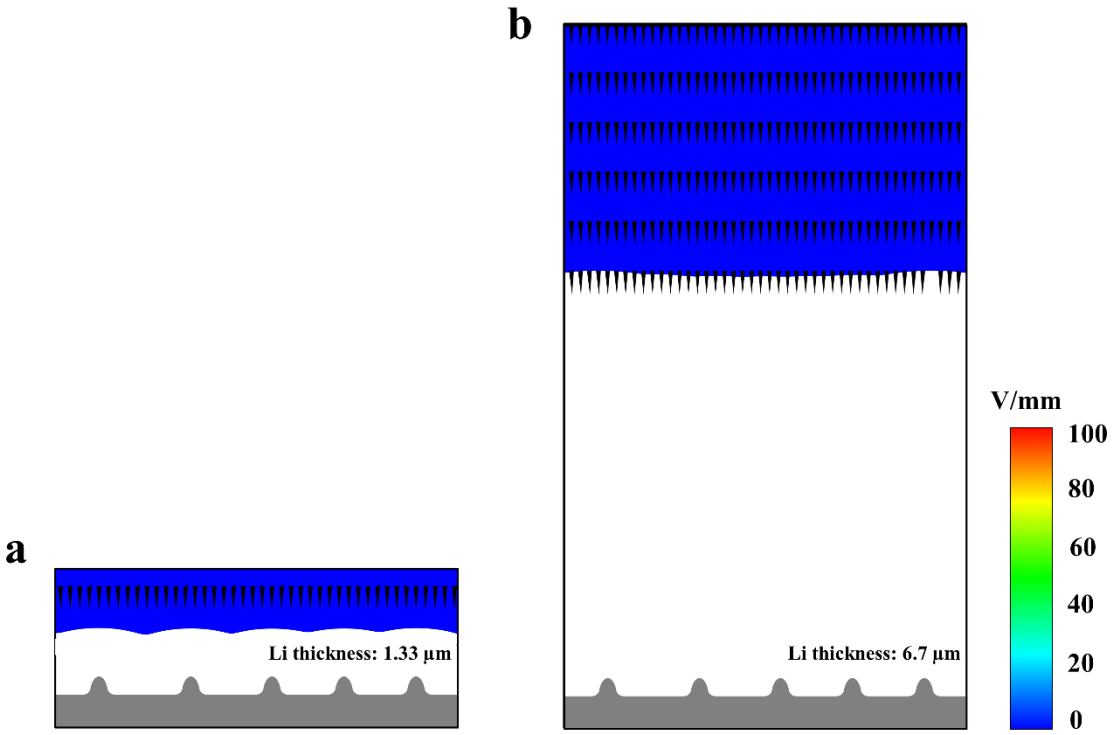

Fig. S2 Potential gradient profile of the Li cell with 2LF2LN electrolyte at the end of the deposition process for 1000 s under the applied current density of (a) 1 mA c m−2 and (b) 5 mA cm−2.

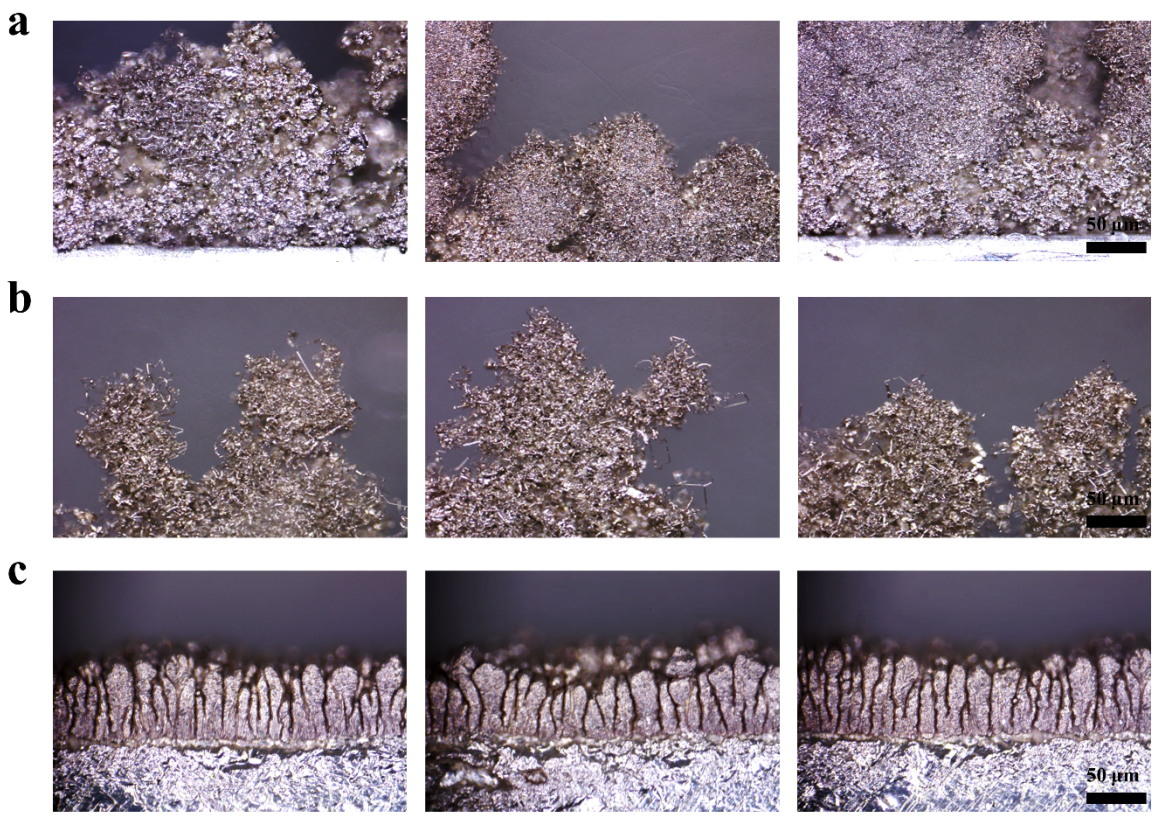

Fig. S3 Final interfacial morphology of the Li metal anode after the electrodeposition for 60 h with (a) 1LTF, (b) 4LF, and (c) 2LF2LN electrolyte systems.

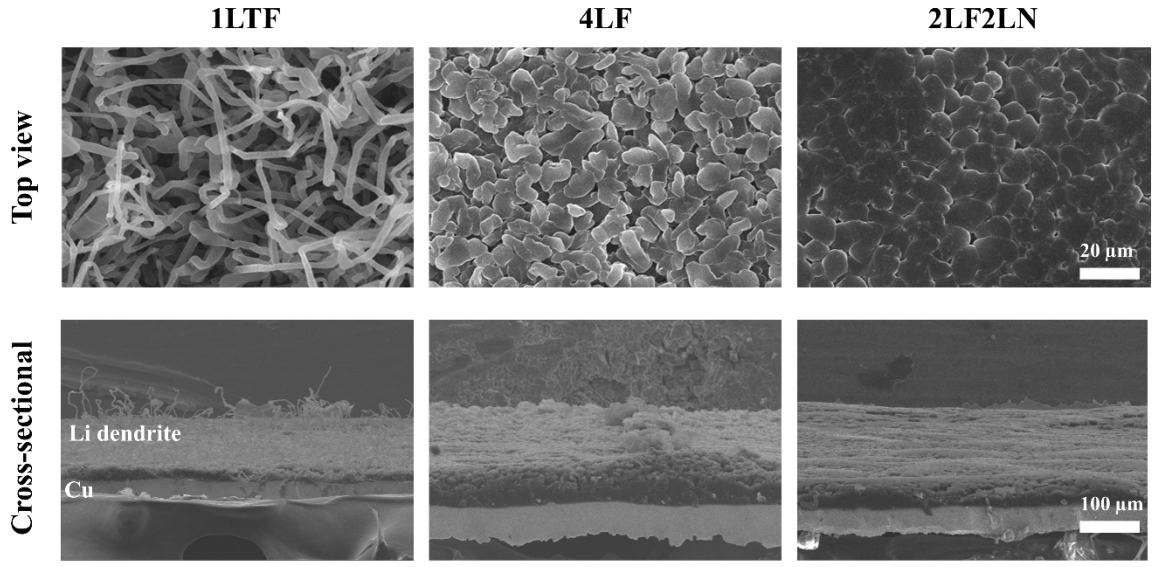

Fig. S4 SEM images at the top and cross-sectional views of the Li metal anode interfacial morphology at the end of the deposition process in the (a) 1LTF, (b) 4LF, and (c) 2LF2LN electrolyte systems.

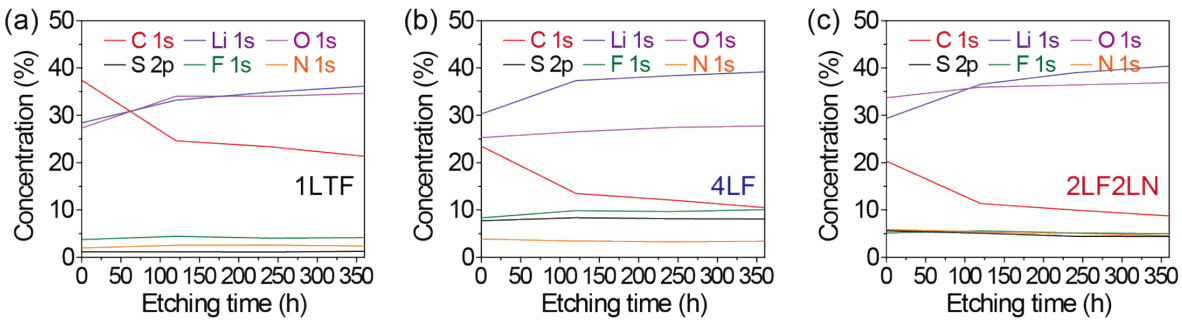

Fig. S6. Variation in elemental distributions in the SEI layer at different Ar+ sputtering times during XPS depth profiling measurements. The samples were prepared by disassembling the Li||Cu cells after the 30th Li stripping in the (a) 1LTF, (b) 4LF, and (c) 2LF2LN electrolytes.

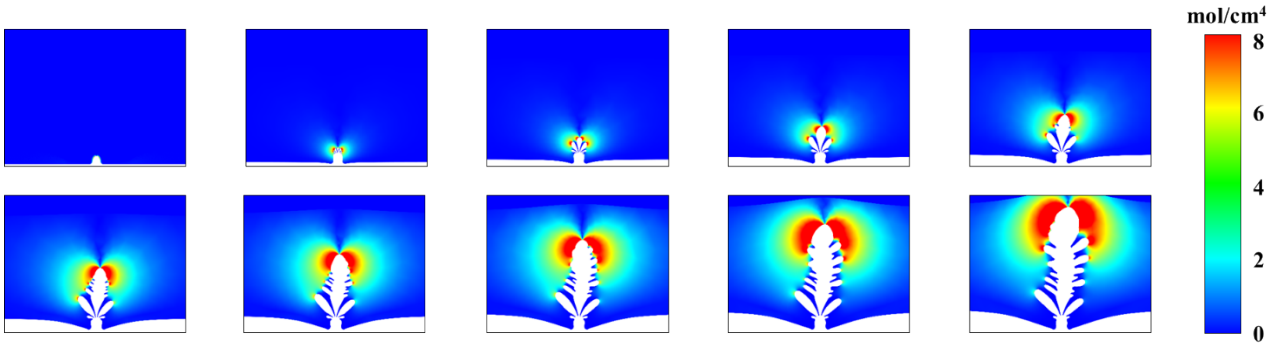

Fig. S6 Evolution of the concentration gradient of the 1 M LiTFSI in DOL/DME with 1% LiNO3 (1LTF) electrolyte systems at 0.25 mA cm−2 in 100 s. The snapshots are obtained at a time step of 100 s.

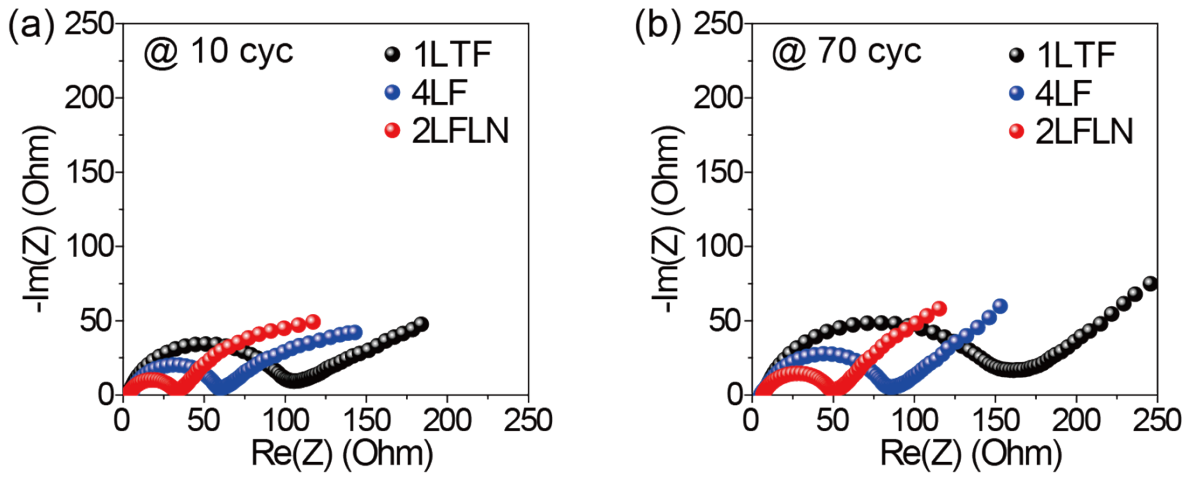

Fig. S7 Nyquist plots for three different electrolyte cells shown in Figure 2j at the 50 and 70th cycle.

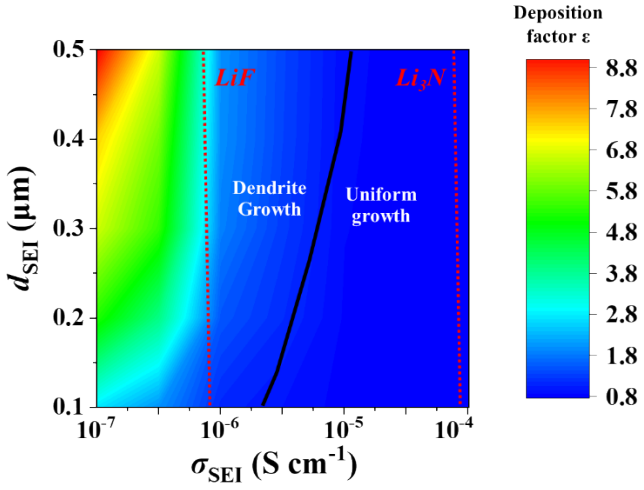

Fig. S8. Contour map of deposition factor as function of ionic conductivity and thick ness of SEI layer.

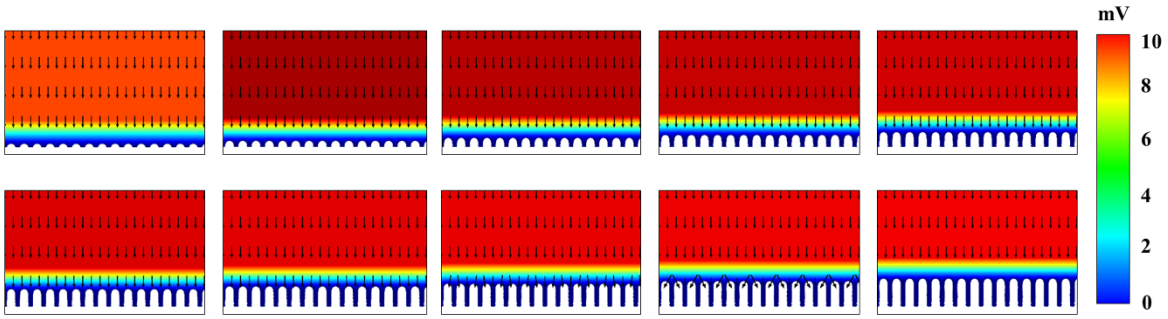

Fig. S9 Geometric evolution of the rod-like dendritic structure of the 2LF2LN electrol yte system at 0.25 mA cm−2 in 1000 s. The snapshots were obtained at a time ste p of 100 s.

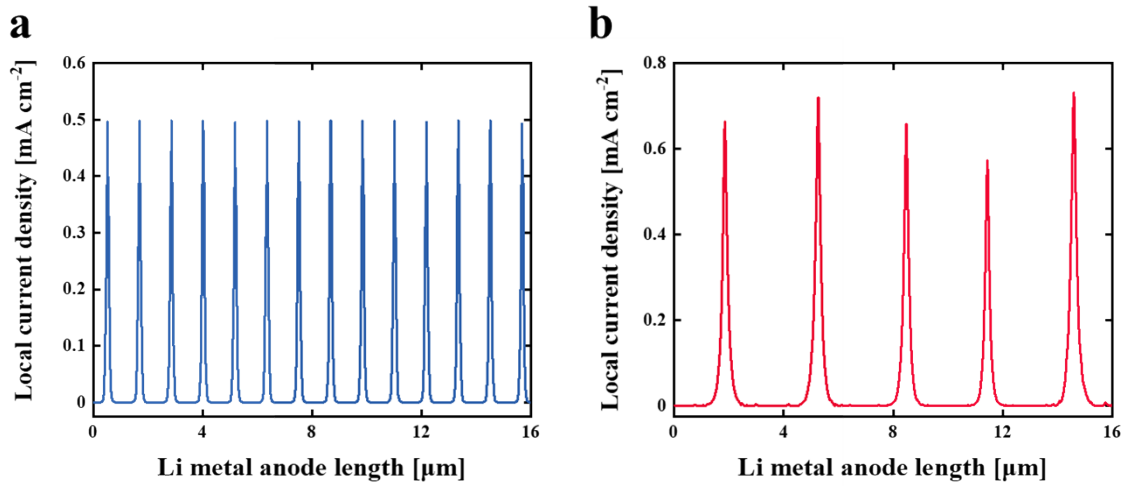

Fig. S10 Local current densities profile of the (a) rod-like dendritic structure and (b) branch-like dendritic structure at 0.25 mA cm−2 at the end of deposition process.

Table S1. Li symmetric cell parameters used in simulation.

Parameters	Symbol	Value
Electrolyte ionic conductivity	σ_{1LTF}	9.678×10^{-3} S cm^{-1}
	σ_{4LF}	3.040×10^{-3} S cm^{-1}
	σ_{2LF2LN}	2.776×10^{-3} S cm^{-1}
Electrolyte diffusion coefficient	D_{1LTF}	1.34×10^{-6} cm^2 s^{-1}
	D_{4LF}	8.03×10^{-7} cm^2 s^{-1}
	D_{2LF2LN}	7.33×10^{-7} cm^2 s^{-1}
SEI ionic conductivity	$\sigma_{SEI@1LTF}$	1.1×10^{-6} S cm^{-1}
	$\sigma_{SEI@4LF}$	1.1×10^{-6} S cm^{-1}
	$\sigma_{SEI@2LF2LN}$	5.0×10^{-3} S cm^{-1}
SEI diffusion coefficient	$D_{SEI@1LTF}$	2.95×10^{-10} cm^2 s^{-1}
	$D_{SEI@4LF}$	2.95×10^{-10} cm^2 s^{-1}
	$D_{SEI@2LF2LN}$	2.68×10^{-7} cm^2 s^{-1}
Cell dimension		110×20 μm
Temperature	T	298 K
Exchange current density	$i_{0@1LTF}$	20.0 mA cm^{-2}
	$i_{0@4LF}$	0.54 mA cm^{-2}
	$i_{0@2LF2LN}$	0.30 mA cm^{-2}
Applied current density	i	0.25–5 mA cm^{-2}
Faraday constant	F	96485 A s mol^{-1}
Gas constant	R	8.314 J K^{-1} mol^{-1}
Molar mass of Li	M	6.941 g mol^{-1}
Density of Li	ρ	534 kg m^{-3}

Table S2. Experimental and theoretical values of Li^+ ionic conductivity in SEI.

Parameters	**Value** [S cm^{-1}]	**Ref**
LiF	1.1×10^{-6}	[1]
LiF-Li_2CO_3	1.7×10^{-6}	[2]
Li_2O	1.05×10^{-6}	[3]
Li_2CO_3	1.02×10^{-6}	[4]
Li_2EDC	2.7×10^{-6}	[5]
Li_3N	$1.0\sim3.21\times10^{-4}$	[6, 7]
Polycrystalline Li_3N	8.06×10^{-4}	[8]
AlI_3-DOL-treated	7.69×10^{-4}	[9]
$AgNO_3$- AMLA	3.33×10^{-3}	[10]
Ethyl α-cyanoacrylate	8.33×10^{-4}	[11]
Tetraethoxysilane	2.5×10^{-3}	[12]
Cu_3N + SBR	4.76×10^{-4}	[13]
PDMS	5.55×10^{-4}	[14]
Al_2O_3 (ALD)	1.0×10^{-4}	[15]
Li-AlF_3	2×10^{-2}	[16]
MXene (Ti3C2Tx)	4.17×10^{-4}	[17]
Li – Hg	4.54×10^{-2}	[18]
1,4-dioxacyclohexane	1.81×10^{-3}	[19]
Li-polyacrylic acid	8.7×10^{-4}	[20]
Li_3PO_4	1.125×10^{-3}	[21]

Computational Model details

For the model validation, input script (M-file format for COMSOL Multiphysic 5.5) for 2LN2LF electrolyte cell was attached as follow:

```
import com.comsol.model.*
import com.comsol.model.util.*

model = ModelUtil.create('Model');

model.modelPath('C:\Users\User\Desktop');

model.label('210527_2LF2LN_1seed.mph');

model.component.create('comp1', true);

model.component('comp1').geom.create('geom1', 2);

model.component('comp1').mesh.create('mesh1');

model.component('comp1').geom('geom1').lengthUnit([native2unicode(hex2dec({
'00' 'b5'}), 'unicode') 'm']);
model.component('comp1').geom('geom1').create('r1', 'Rectangle');
model.component('comp1').geom('geom1').feature('r1').label('El');
model.component('comp1').geom('geom1').feature('r1').set('pos', [0 1.5]);
model.component('comp1').geom('geom1').feature('r1').set('size', [20 50]);
model.component('comp1').geom('geom1').create('r2', 'Rectangle');
model.component('comp1').geom('geom1').feature('r2').label('SEI');
model.component('comp1').geom('geom1').feature('r2').set('pos', [0 0]);
model.component('comp1').geom('geom1').feature('r2').set('size', [20 1.5]);
model.component('comp1').geom('geom1').create('e1', 'Ellipse');
model.component('comp1').geom('geom1').feature('e1').label('seed');
model.component('comp1').geom('geom1').feature('e1').set('pos', {'10-
0.0625' '0'});
model.component('comp1').geom('geom1').feature('e1').set('semiaxes',
[0.0625 0.125]);
model.component('comp1').geom('geom1').create('dif1', 'Difference');
model.component('comp1').geom('geom1').feature('dif1').set('intbnd', false);
model.component('comp1').geom('geom1').feature('dif1').selection('input').s
et({'r2'});
model.component('comp1').geom('geom1').feature('dif1').selection('input2').
set({'e1'});
model.component('comp1').geom('geom1').create('r3', 'Rectangle');
model.component('comp1').geom('geom1').feature('r3').label('couter
electrode');
model.component('comp1').geom('geom1').feature('r3').set('pos', [0 51.5]);
model.component('comp1').geom('geom1').feature('r3').set('size', [20 30]);
model.component('comp1').geom('geom1').create('r4', 'Rectangle');
model.component('comp1').geom('geom1').feature('r4').label('working
eledtrode ');
model.component('comp1').geom('geom1').feature('r4').set('pos', [0 -28.5]);
model.component('comp1').geom('geom1').feature('r4').set('size', [20 30]);
model.component('comp1').geom('geom1').create('fil1', 'Fillet');
model.component('comp1').geom('geom1').feature('fil1').set('radius', 0.05);
model.component('comp1').geom('geom1').feature('fil1').selection('point').s
```

```
et('dif1(1)', 3);
model.component('comp1').geom('geom1').create('fil2', 'Fillet');
model.component('comp1').geom('geom1').feature('fil2').set('radius', 0.05);
model.component('comp1').geom('geom1').feature('fil2').selection('point').s
et('fil1(1)', 6);
model.component('comp1').geom('geom1').feature('fin').set('repairtoltype',
'relative');
model.component('comp1').geom('geom1').run;
model.component('comp1').geom('geom1').run('fin');

model.component('comp1').material.create('mat1', 'Common');
model.component('comp1').material('mat1').selection.set([1 4]);
model.component('comp1').material('mat1').propertyGroup('def').func.create(
'k_solid_1', 'Piecewise');
model.component('comp1').material('mat1').propertyGroup('def').func.create(
'res_solid_1', 'Piecewise');
model.component('comp1').material('mat1').propertyGroup('def').func.create(
'alpha_solid_1', 'Piecewise');
model.component('comp1').material('mat1').propertyGroup('def').func.create(
'C_solid_1', 'Piecewise');
model.component('comp1').material('mat1').propertyGroup('def').func.create(
'sigma_solid_1', 'Piecewise');
model.component('comp1').material('mat1').propertyGroup('def').func.create(
'HC_solid_1', 'Piecewise');
model.component('comp1').material('mat1').propertyGroup('def').func.create(
'VP_solid_1', 'Piecewise');
model.component('comp1').material('mat1').propertyGroup('def').func.create(
'rho_solid_1', 'Piecewise');
model.component('comp1').material('mat1').propertyGroup('def').func.create(
'TD', 'Piecewise');
model.component('comp1').material('mat1').propertyGroup.create('ThermalExpa
nsion', 'Thermal expansion');
model.component('comp1').material('mat1').propertyGroup('ThermalExpansion').f
unc.create('dL_solid_1', 'Piecewise');
model.component('comp1').material('mat1').propertyGroup.create('Enu',
'Young''s modulus and Poisson''s ratio');
model.component('comp1').material('mat1').propertyGroup('Enu').func.create(
'E', 'Piecewise');
model.component('comp1').material('mat1').propertyGroup('Enu').func.create(
'nu', 'Piecewise');
model.component('comp1').material('mat1').propertyGroup.create('KG', 'Bulk
modulus and shear modulus');
model.component('comp1').material('mat1').propertyGroup('KG').func.create('
mu', 'Piecewise');
model.component('comp1').material('mat1').propertyGroup('KG').func.create('
kappa_solid_1', 'Piecewise');

model.component('comp1').physics.create('liion', 'LithiumIonBatteryMPH',
'geom1');
model.component('comp1').physics('liion').create('ece1', 'Electrode', 2);
model.component('comp1').physics('liion').feature('ece1').selection.set([4]);

model.component('comp1').physics('liion').create('ece2', 'Electrode', 2);
model.component('comp1').physics('liion').feature('ece2').selection.set([1]);

model.component('comp1').physics('liion').create('bei1',
'InternalElectrodeSurface', 1);
model.component('comp1').physics('liion').feature('bei1').selection.set([8]);
```

```
model.component('comp1').physics('liion').create('bei2',
'InternalElectrodeSurface', 1);
model.component('comp1').physics('liion').feature('bei2').selection.set([4
10 15 16 17 18]);
model.component('comp1').physics('liion').create('egnd1', 'ElectricGround',
1);
model.component('comp1').physics('liion').feature('egnd1').selection.set([2])
;
model.component('comp1').physics('liion').create('ecd1',
'ElectrodeNormalCurrentDensity', 1);
model.component('comp1').physics('liion').feature('ecd1').selection.set([9]);

model.component('comp1').physics('liion').create('ice2', 'Electrolyte', 2);
model.component('comp1').physics('liion').feature('ice2').selection.set([2]);

model.component('comp1').physics.create('dg', 'DeformedGeometry', 'geom1');
model.component('comp1').physics('dg').create('free1', 'FreeDeformation',
2);
model.component('comp1').physics('dg').feature('free1').selection.all;

model.component('comp1').multiphysics.create('ndb1', 'NonDeformingBoundary',
1);
model.component('comp1').multiphysics('ndb1').selection.set([1 2 3 5 7 9 11
12 13 14]);
model.component('comp1').multiphysics.create('des1',
'DeformingElectrodeSurface', 1);
model.component('comp1').multiphysics('des1').selection.set([4 8 10 15 16
17 18]);

model.component('comp1').mesh('mesh1').create('ftri1', 'FreeTri');
model.component('comp1').mesh('mesh1').feature('ftri1').create('dis1',
'Distribution');
model.component('comp1').mesh('mesh1').feature('ftri1').feature('dis1').sel
ection.set([16 17]);

model.component('comp1').view('view1').axis.set('xmin', 9.321166038513184);
model.component('comp1').view('view1').axis.set('xmax', 10.559062957763672);
model.component('comp1').view('view1').axis.set('ymin', -
0.2201368808746338);
model.component('comp1').view('view1').axis.set('ymax', 0.6915667057037354);

model.component('comp1').material('mat1').label('Lithium [solid]');
model.component('comp1').material('mat1').set('family', 'custom');
model.component('comp1').material('mat1').set('specular', 'custom');
model.component('comp1').material('mat1').set('customspecular',
[0.7843137254901961 1 1]);
model.component('comp1').material('mat1').set('diffuse', 'custom');
model.component('comp1').material('mat1').set('customdiffuse',
[0.7843137254901961 0.7843137254901961 0.7843137254901961]);
model.component('comp1').material('mat1').set('ambient', 'custom');
model.component('comp1').material('mat1').set('customambient',
[0.7843137254901961 0.7843137254901961 0.7843137254901961]);
model.component('comp1').material('mat1').set('noise', true);
model.component('comp1').material('mat1').set('noisefreq', 1);
model.component('comp1').material('mat1').set('lighting', 'cooktorrance');
model.component('comp1').material('mat1').set('fresnel', 0.9);
model.component('comp1').material('mat1').propertyGroup('def').func('k_soli
```

```
d_1').set('arg', 'T');
model.component('comp1').material('mat1').propertyGroup('def').func('k_soli
d_1').set('pieces', {'0.0' '20.0' '59.12757*T^1+3.00429*T^2-
0.3623115*T^3+0.008408706*T^4-3.573711E-5*T^5'; ...
'20.0' '60.0' '-96.1324+144.0682*T^1-8.233173*T^2+0.191246*T^3-
0.002053514*T^4+8.449728E-6*T^5'; ...
'60.0' '120.0' '1233.451-37.96573*T^1+0.4816627*T^2-
0.002724229*T^3+5.754475E-6*T^4'; ...
'120.0' '454.0' '157.4963-0.9481831*T^1+0.005657717*T^2-1.814768E-
5*T^3+2.961967E-8*T^4-1.95023E-11*T^5'});
model.component('comp1').material('mat1').propertyGroup('def').func('res_so
lid_1').set('arg', 'T');
model.component('comp1').material('mat1').propertyGroup('def').func('res_so
lid_1').set('pieces', {'1.0' '8.0' '7.235714E-11+9.209957E-14*T^1-7.5E-
14*T^2+2.424242E-14*T^3-1.515152E-15*T^4'; ...
'8.0' '30.0' '5.621684E-11+4.538199E-12*T^1-4.289635E-13*T^2+1.829223E-
14*T^3'; ...
'30.0' '60.0' '-2.85605E-9+2.445621E-10*T^1-6.966874E-12*T^2+7.73913E-
14*T^3'; ...
'60.0' '454.0' '-1.468938E-8+2.516884E-10*T^1+1.009909E-12*T^2-2.927657E-
15*T^3+2.888384E-18*T^4'});
model.component('comp1').material('mat1').propertyGroup('def').func('alpha_
solid_1').set('arg', 'T');
model.component('comp1').material('mat1').propertyGroup('def').func('alpha_
solid_1').set('pieces', {'0.0' '388.0' '2.680594E-5+9.446291E-
8*T^1+3.562978E-10*T^2-3.996191E-12*T^3+1.154477E-14*T^4-1.093958E-
17*T^5'});
model.component('comp1').material('mat1').propertyGroup('def').func('C_soli
d_1').set('arg', 'T');
model.component('comp1').material('mat1').propertyGroup('def').func('C_soli
d_1').set('pieces', {'0.0' '5.0' '0.2807509*T^1-
0.03148414*T^2+0.01212677*T^3'; ...
'5.0' '40.0' '-1.482961+0.9201118*T^1-0.09668396*T^2+0.01204451*T^3-
1.160699E-4*T^4'; ...
'40.0' '140.0' '145.9123-19.22309*T^1+0.8336812*T^2-
0.006158287*T^3+1.46552E-5*T^4'; ...
'140.0' '453.6' '-1127.176+44.33086*T^1-0.1689252*T^2+3.04063E-4*T^3-
1.97783E-7*T^4'});
model.component('comp1').material('mat1').propertyGroup('def').func('sigma_
solid_1').set('arg', 'T');
model.component('comp1').material('mat1').propertyGroup('def').func('sigma_
solid_1').set('pieces', {'1.0' '8.0' '1/(-1.515152E-15*T^4+2.424242E-
14*T^3-7.500000E-14*T^2+9.209957E-14*T+7.235714E-11)'; ...
'8.0' '30.0' '1/(1.829223E-14*T^3-4.289635E-13*T^2+4.538199E-
12*T+5.621684E-11)'; ...
'30.0' '60.0' '1/(7.739130E-14*T^3-6.966874E-12*T^2+2.445621E-10*T-
2.85605E-09)'; ...
'60.0' '454.0' '1/(2.888384E-18*T^4-2.927657E-15*T^3+1.009909E-
12*T^2+2.516884E-10*T-1.468938E-08)'});
model.component('comp1').material('mat1').propertyGroup('def').func('HC_sol
id_1').set('arg', 'T');
model.component('comp1').material('mat1').propertyGroup('def').func('HC_sol
id_1').set('pieces', {'0.0' '5.0' '0.001948692*T^1-2.185314E-
4*T^2+8.417191E-5*T^3'; ...
'5.0' '40.0' '-0.01029323+0.006386495*T^1-6.710835E-4*T^2+8.360096E-5*T^3-
8.056413E-7*T^4'; ...
'40.0' '140.0' '1.012777-0.1334275*T^1+0.005786581*T^2-4.274466E-
5*T^3+1.017218E-7*T^4'; ...
'140.0' '453.6' '-7.823729+0.3077005*T^1-0.00117251*T^2+2.110501E-6*T^3-
```

```
1.372812E-9*T^4'});
model.component('comp1').material('mat1').propertyGroup('def').func('VP_sol
id_1').set('arg', 'T');
model.component('comp1').material('mat1').propertyGroup('def').func('VP_sol
id_1').set('pieces', {'293.0' '454.0' '(exp((-
8.310000e+03/T+8.547810e+00)*log(10.0)))*1.333200e+02'});
model.component('comp1').material('mat1').propertyGroup('def').func('rho_so
lid_1').set('arg', 'T');
model.component('comp1').material('mat1').propertyGroup('def').func('rho_so
lid_1').set('pieces', {'0.0' '100.0' '547.8209-1.171171E-4*T^1+3.671277E-
5*T^2-2.437039E-6*T^3+9.765011E-9*T^4-1.225737E-11*T^5'; '100.0' '388.0'
'546.7914+0.03822972*T^1-4.974667E-4*T^2+1.044225E-6*T^3-8.90107E-10*T^4'});
model.component('comp1').material('mat1').propertyGroup('def').func('TD').s
et('arg', 'T');
model.component('comp1').material('mat1').propertyGroup('def').func('TD').s
et('pieces', {'3.0' '14.0' '0.6796846-0.1173027*T^1+0.009700871*T^2-
4.417159E-4*T^3+9.405466E-6*T^4-4.654822E-8*T^5'; ...
'14.0' '27.0' '0.5862995-0.08315858*T^1+0.005058256*T^2-1.616193E-
4*T^3+2.676131E-6*T^4-1.82034E-8*T^5'; ...
'27.0' '52.0' '0.2467828-0.0252109*T^1+0.001071106*T^2-2.334033E-
5*T^3+2.586354E-7*T^4-1.159014E-9*T^5'; ...
'52.0' '92.0' '0.03111304-0.001866731*T^1+4.619279E-5*T^2-5.813458E-
7*T^3+3.695173E-9*T^4-9.447155E-12*T^5'; ...
'92.0' '200.0' '0.001550711-4.301493E-5*T^1+5.131035E-7*T^2-3.105545E-
9*T^3+9.420941E-12*T^4-1.139711E-14*T^5'; ...
'200.0' '388.0' '1.644233E-4-1.225272E-6*T^1+4.998337E-9*T^2-9.541854E-
12*T^3+6.852377E-15*T^4'});
model.component('comp1').material('mat1').propertyGroup('def').set('thermal
conductivity', {'k_solid_1(T[1/K])[W/(m*K)]' '0' '0' '0'
'k_solid_1(T[1/K])[W/(m*K)]' '0' '0' '0' 'k_solid_1(T[1/K])[W/(m*K)]'});
model.component('comp1').material('mat1').propertyGroup('def').set('resisti
vity', {'res_solid_1(T[1/K])[ohm*m]' '0' '0' '0'
'res_solid_1(T[1/K])[ohm*m]' '0' '0' '0' 'res_solid_1(T[1/K])[ohm*m]'});
model.component('comp1').material('mat1').propertyGroup('def').set('thermal
expansioncoefficient', {'(alpha_solid_1(T[1/K])[1/K]+(Tempref-
293[K])*if(abs(T-Tempref)>1e-3,(alpha_solid_1(T[1/K])[1/K]-
alpha_solid_1(Tempref[1/K])[1/K])/(T-
Tempref),d(alpha_solid_1(T[1/K])[1/K],T)))/(1+alpha_solid_1(Tempref[1/K])[1
/K]*(Tempref-293[K]))' '0' '0' '0' '(alpha_solid_1(T[1/K])[1/K]+(Tempref-
293[K])*if(abs(T-Tempref)>1e-3,(alpha_solid_1(T[1/K])[1/K]-
alpha_solid_1(Tempref[1/K])[1/K])/(T-
Tempref),d(alpha_solid_1(T[1/K])[1/K],T)))/(1+alpha_solid_1(Tempref[1/K])[1
/K]*(Tempref-293[K]))' '0' '0' '0' '(alpha_solid_1(T[1/K])[1/K]+(Tempref-
293[K])*if(abs(T-Tempref)>1e-3,(alpha_solid_1(T[1/K])[1/K]-
alpha_solid_1(Tempref[1/K])[1/K])/(T-
Tempref),d(alpha_solid_1(T[1/K])[1/K],T)))/(1+alpha_solid_1(Tempref[1/K])[1
/K]*(Tempref-293[K]))'});
model.component('comp1').material('mat1').propertyGroup('def').set('heatcap
acity', 'C_solid_1(T[1/K])[J/(kg*K)]');
model.component('comp1').material('mat1').propertyGroup('def').set('electri
cconductivity', {'sigma_solid_1(T[1/K])[S/m]' '0' '0' '0'
'sigma_solid_1(T[1/K])[S/m]' '0' '0' '0' 'sigma_solid_1(T[1/K])[S/m]'});
model.component('comp1').material('mat1').propertyGroup('def').set('HC',
'HC_solid_1(T[1/K])[J/(mol*K)]');
model.component('comp1').material('mat1').propertyGroup('def').set('VP',
'VP_solid_1(T[1/K])[Pa]');
model.component('comp1').material('mat1').propertyGroup('def').set('density
', 'rho_solid_1(T[1/K])[kg/m^3]');
model.component('comp1').material('mat1').propertyGroup('def').set('TD',
```

```
'TD(T[1/K])[m^2/s]');
model.component('comp1').material('mat1').propertyGroup('def').addInput('te
mperature');
model.component('comp1').material('mat1').propertyGroup('def').addInput('st
rainreferencetemperature');
model.component('comp1').material('mat1').propertyGroup('ThermalExpansion').f
unc('dL_solid_1').set('arg', 'T');
model.component('comp1').material('mat1').propertyGroup('ThermalExpansion').f
unc('dL_solid_1').set('pieces', {'0.0' '240.0' '-0.007862787+7.041071E-
8*T^1-2.213372E-8*T^2+1.470315E-9*T^3-5.889381E-12*T^4+7.517221E-15*T^5';
'240.0' '388.0' '-0.01066377+2.673472E-5*T^1+3.297059E-8*T^2'});
model.component('comp1').material('mat1').propertyGroup('ThermalExpansion').s
et('alphatan', '');
model.component('comp1').material('mat1').propertyGroup('ThermalExpansion').s
et('dL', '');
model.component('comp1').material('mat1').propertyGroup('ThermalExpansion').s
et('alphatanIso', '');
model.component('comp1').material('mat1').propertyGroup('ThermalExpansion').s
et('dLIso', '');
model.component('comp1').material('mat1').propertyGroup('ThermalExpansion').s
et('dL', {'(dL_solid_1(T[1/K])-
dL_solid_1(Tempref[1/K]))/(1+dL_solid_1(Tempref[1/K]))' '0' '0' '0'
'(dL_solid_1(T[1/K])-
dL_solid_1(Tempref[1/K]))/(1+dL_solid_1(Tempref[1/K]))' '0' '0' '0'
'(dL_solid_1(T[1/K])-
dL_solid_1(Tempref[1/K]))/(1+dL_solid_1(Tempref[1/K]))'});
model.component('comp1').material('mat1').propertyGroup('ThermalExpansion').s
et('dLIso', '(dL_solid_1(T)-dL_solid_1(Tempref))/(1+dL_solid_1(Tempref))');
model.component('comp1').material('mat1').propertyGroup('ThermalExpansion').a
ddInput('temperature');
model.component('comp1').material('mat1').propertyGroup('ThermalExpansion').a
ddInput('strainreferencetemperature');
model.component('comp1').material('mat1').propertyGroup('Enu').func('E').se
t('arg', 'T');
model.component('comp1').material('mat1').propertyGroup('Enu').func('E').se
t('pieces', {'78.0' '298.0' '1.27027E10-1.263836E7*T^1+12088.85*T^2'});
model.component('comp1').material('mat1').propertyGroup('Enu').func('nu').s
et('arg', 'T');
model.component('comp1').material('mat1').propertyGroup('Enu').func('nu').s
et('pieces', {'78.0' '298.0' '0.3310383-7.152841E-5*T^1+2.707221E-
7*T^2+2.93754E-10*T^3'});
model.component('comp1').material('mat1').propertyGroup('Enu').set('youngsm
odulus', 'E(T[1/K])[Pa]');
model.component('comp1').material('mat1').propertyGroup('Enu').set('poisson
sratio', 'nu(T[1/K])');
model.component('comp1').material('mat1').propertyGroup('Enu').addInput('te
mperature');
model.component('comp1').material('mat1').propertyGroup('KG').func('mu').se
t('arg', 'T');
model.component('comp1').material('mat1').propertyGroup('KG').func('mu').se
t('pieces', {'78.0' '298.0' '4.771964E9-4496430.0*T^1+3364.486*T^2'});
model.component('comp1').material('mat1').propertyGroup('KG').func('kappa_s
olid_1').set('arg', 'T');
model.component('comp1').material('mat1').propertyGroup('KG').func('kappa_s
olid_1').set('pieces', {'78.0' '298.0' '1.245888E10-
1.603332E7*T^1+25154.2*T^2+23.06149*T^3'});
model.component('comp1').material('mat1').propertyGroup('KG').set('K', '');
model.component('comp1').material('mat1').propertyGroup('KG').set('G', '');
model.component('comp1').material('mat1').propertyGroup('KG').set('K',
```

```
'kappa_solid_1(T[1/K])[Pa]');
model.component('comp1').material('mat1').propertyGroup('KG').set('G',
'mu(T[1/K])[Pa]');
model.component('comp1').material('mat1').propertyGroup('KG').addInput('tem
perature');

model.common('cminpt').label('Common model inputs 1');

model.component('comp1').physics('liion').prop('ShapeProperty').set('order_
electricpotential', 1);
model.component('comp1').physics('liion').feature('ice1').set('sigmal',
{'3e-3[S/cm]'; '0'; '0'; '0'; '3e-3[S/cm]'; '0'; '0'; '0'; '3e-3[S/cm]'});
model.component('comp1').physics('liion').feature('ice1').set('Dl', '8.03e-
7[cm^2/s]');
model.component('comp1').physics('liion').feature('init1').set('cl',
'4000[mol/m^3]');
model.component('comp1').physics('liion').feature('bei1').set('Species',
's1');
model.component('comp1').physics('liion').feature('bei1').set('Ms',
0.006941);
model.component('comp1').physics('liion').feature('bei1').set('rhos', 534);
model.component('comp1').physics('liion').feature('bei1').feature('er1').se
t('ElectrodeKinetics', 'ButlerVolmer');
model.component('comp1').physics('liion').feature('bei1').feature('er1').se
t('i0', '54[mA/cm^2]');
model.component('comp1').physics('liion').feature('bei2').set('Species',
's1');
model.component('comp1').physics('liion').feature('bei2').set('Ms',
0.006941);
model.component('comp1').physics('liion').feature('bei2').set('rhos', 534);
model.component('comp1').physics('liion').feature('bei2').feature('er1').se
t('ElectrodeKinetics', 'ButlerVolmer');
model.component('comp1').physics('liion').feature('bei2').feature('er1').se
t('i0', '54[mA/cm^2]');
model.component('comp1').physics('liion').feature('ecd1').set('nis',
'0.25[mA/cm^2]');
model.component('comp1').physics('liion').feature('ice2').set('sigmal',
{'1.1e-3[S/cm]'; '0'; '0'; '0'; '1.1e-3[S/cm]'; '0'; '0'; '0'; '1.1e-
3[S/cm]'});
model.component('comp1').physics('liion').feature('ice2').set('Dl', '2.68e-
7[cm^2/s]');
model.component('comp1').physics('liion').feature('ice2').label('SEI
(Li3N)');
model.component('comp1').physics('dg').prop('FrameSettings').set('geometryS
hapeOrder', 1);
model.component('comp1').physics('dg').prop('FreeDeformationSettings').set(
'smoothingType', 'hyperelastic');
model.component('comp1').physics('dg').feature('disp1').set('useDx', [0;
0]);

model.component('comp1').multiphysics('ndb1').set('BoundaryCondition',
'ZeroNormalDisplacement');

model.component('comp1').mesh('mesh1').feature('ftri1').feature('dis1').set
('numelem', 200);
model.component('comp1').mesh('mesh1').run;

model.component('comp1').physics('liion').feature('ice1').set('sigmal_mat',
```

```
'userdef');
model.component('comp1').physics('liion').feature('ice1').set('transpNum_ma
t', 'userdef');
model.component('comp1').physics('liion').feature('ice1').set('fcl_mat',
'userdef');
model.component('comp1').physics('liion').feature('bei1').feature('er1').se
t('Eeq_mat', 'userdef');
model.component('comp1').physics('liion').feature('bei1').feature('er1').se
t('dEeqdT_mat', 'userdef');
model.component('comp1').physics('liion').feature('bei2').feature('er1').se
t('Eeq_mat', 'userdef');
model.component('comp1').physics('liion').feature('bei2').feature('er1').se
t('dEeqdT_mat', 'userdef');
model.component('comp1').physics('liion').feature('ice2').set('sigmal_mat',
'userdef');
model.component('comp1').physics('liion').feature('ice2').set('transpNum_ma
t', 'userdef');
model.component('comp1').physics('liion').feature('ice2').set('fcl_mat',
'userdef');

model.study.create('std1');
model.study('std1').create('time', 'Transient');

model.sol.create('sol1');
model.sol('sol1').study('std1');
model.sol('sol1').attach('std1');
model.sol('sol1').create('st1', 'StudyStep');
model.sol('sol1').create('v1', 'Variables');
model.sol('sol1').create('t1', 'Time');
model.sol('sol1').feature('t1').create('arDef', 'AutoRemesh');
model.sol('sol1').feature('t1').create('fc1', 'FullyCoupled');
model.sol('sol1').feature('t1').create('d1', 'Direct');
model.sol('sol1').feature('t1').feature.remove('fcDef');
model.sol.create('sol2');
model.sol('sol2').study('std1');

model.result.dataset.remove('dset1');
model.result.dataset.remove('dset2');

model.study('std1').feature('time').set('tlist', 'range(0,0.5,1000)');
model.study('std1').feature('time').set('plot', true);
model.study('std1').feature('time').set('autoremesh', true);

model.sol('sol1').attach('std1');
model.sol('sol1').feature('v1').set('resscalemethod', 'auto');
model.sol('sol1').feature('v1').set('clist', {'range(0,0.5,1000)'
'1.0[s]'});
model.sol('sol1').feature('v1').feature('comp1_cl').set('scalemethod',
'manual');
model.sol('sol1').feature('v1').feature('comp1_cl').set('scaleval', 1000);
model.sol('sol1').feature('v1').feature('comp1_material_disp').set('scaleme
thod', 'manual');
model.sol('sol1').feature('v1').feature('comp1_material_disp').set('scaleva
l', 6.972452939963094E-10);
model.sol('sol1').feature('v1').feature('comp1_material_lm_nv').set('out',
false);
model.sol('sol1').feature('v1').feature('comp1_phil').set('scalemethod',
'manual');
```

```
model.sol('sol1').feature('v1').feature('comp1_phil').set('scaleval', 1);
model.sol('sol1').feature('v1').feature('comp1_phis').set('scalemethod',
'manual');
model.sol('sol1').feature('v1').feature('comp1_phis').set('scaleval', 1);
model.sol('sol1').feature('t1').set('control', 'user');
model.sol('sol1').feature('t1').set('tlist', 'range(0,0.5,1000)');
model.sol('sol1').feature('t1').set('rtol', 0.001);
model.sol('sol1').feature('t1').set('maxorder', 2);
model.sol('sol1').feature('t1').set('plot', true);
model.sol('sol1').feature('t1').set('eventout', true);
model.sol('sol1').feature('t1').feature('arDef').set('stopexpr',
'min(comp1.material.minqual-0.2,min(comp1.material.minqual-
0.4,min(comp1.material.minqual-0.4,min(comp1.material.minqual-
0.4,min(comp1.material.minqual-0.4,min(comp1.material.minqual-
0.4,comp1.material.minqual-0.4))))))');
model.sol('sol1').feature('t1').feature('arDef').set('stopval', '0');
model.sol('sol1').feature('t1').feature('arDef').set('consistentremesh',
'bweuler');
model.sol('sol1').feature('t1').feature('arDef').set('tadapsol', 'sol2');
model.sol('sol1').feature('t1').feature('arDef').set('tadapmesh', {'mesh2'
'mesh3' 'mesh4' 'mesh5'});
model.sol('sol1').feature('t1').feature('fc1').set('dtech', 'auto');
model.sol('sol1').feature('t1').feature('fc1').set('maxiter', 5);
model.sol('sol1').feature('t1').feature('d1').set('mumpsalloc', 1.4);
model.sol('sol1').runAll;
model.sol('sol2').label('Remeshed Solution 1');
model.sol('sol2').runAll;
```

References

[1] J. Pan, Q. Zhang, X. Xiao, Y.T. Cheng, Y. Qi, Design of Nanostructured Heterogeneous Solid Ionic Coatings through a Multiscale Defect Model, ACS Appl. Mater. Interfaces. 8 (2016) 5687–5693. https://doi.org/10.1021/acsami.5b12030.

[2] A. Ramasubramanian, V. Yurkiv, T. Foroozan, M. Ragone, R. Shahbazian-Yassar, F. Mashayek, Lithium Diffusion Mechanism through Solid-Electrolyte Interphase in Rechargeable Lithium Batteries, J. Phys. Chem. C. 123 (2019) 10237–10245. https://doi.org/10.1021/acs.jpcc.9b00436.

[3] O. Borodin, G.D. Smith, P. Fan, Molecular dynamics simulations of lithium alkyl carbonates, J. Phys. Chem. B. 110 (2006) 22773–22779. https://doi.org/10.1021/jp0639142.

[4] J.-I. Lee, S. Cho, T.T. Vu, S. Kim, S. Ryu, J. Moon, S. Park, Hybrid polyion complex micelles enabling high-performance lithium-metal batteries with universal carbonates, Energy Storage Materials. 38 (2021) 509–519. https://doi.org/10.1016/j.ensm.2021.04.001.

[5] H. Wu, Y. Cao, L. Geng, C. Wang, In Situ Formation of Stable Interfacial Coating for High Performance Lithium Metal Anodes, Chem. Mater. 29 (2017) 3572–3579. https://doi.org/10.1021/acs.chemmater.6b05475.

[6] Q.C. Liu, J.J. Xu, S. Yuan, Z.W. Chang, D. Xu, Y. Bin Yin, L. Li, H.X. Zhong, Y.S. Jiang, J.M. Yan, X.B. Zhang, Artificial Protection Film on Lithium Metal Anode toward Long-Cycle-Life Lithium-Oxygen Batteries, Adv. Mater. 27 (2015) 5241–5247. https://doi.org/10.1002/adma.201501490.

[7] B. Thirumalraj, T.T. Hagos, C.J. Huang, M.A. Teshager, J.H. Cheng, W.N. Su, B.J. Hwang, Nucleation and Growth Mechanism of Lithium Metal Electroplating, J. Am. Chem. Soc. 141 (2019) 18612–18623. https://doi.org/10.1021/jacs.9b10195.

[8] N.S. Choi, Y.M. Lee, W. Seol, J.A. Lee, J.K. Park, Protective coating of lithium metal electrode for interfacial enhancement with gel polymer electrolyte, Solid State Ionics. 172 (2004) 19–24. https://doi.org/10.1016/j.ssi.2004.05.008.

[9] B. Thirumalraj, T.T. Hagos, C.J. Huang, M.A. Teshager, J.H. Cheng, W.N. Su, B.J. Hwang, Nucleation and Growth Mechanism of Lithium Metal Electroplating, J. Am. Chem. Soc. 141 (2019) 18612–18623. https://doi.org/10.1021/jacs.9b10195.

[10] N.S. Choi, Y.M. Lee, W. Seol, J.A. Lee, J.K. Park, Protective coating of lithium metal electrode for interfacial enhancement with gel polymer electrolyte, Solid State Ionics. 172 (2004) 19–24. https://doi.org/10.1016/j.ssi.2004.05.008.

[11] J. Gu, C. Shen, Z. Fang, J. Yu, Y. Zheng, Z. Tian, L. Shao, X. Li, K. Xie, Toward High-Performance Li Metal Anode via Difunctional Protecting Layer, Front. Chem. 7 (2019) 1–9. https://doi.org/10.3389/fchem.2019.00572.

[12] Z. Hu, S. Zhang, S. Dong, W. Li, H. Li, G. Cui, L. Chen, Poly(ethyl α-cyanoacrylate)-Based Artificial Solid Electrolyte Interphase Layer for Enhanced Interface Stability of Li Metal Anodes, Chem. Mater. 29 (2017) 4682–4689. https://doi.org/10.1021/acs.chemmater.7b00091.

[13] G.A. Umeda, E. Menke, M. Richard, K.L. Stamm, F. Wudl, B. Dunn, Protection of lithium metal surfaces using tetraethoxysilane, J. Mater. Chem. 21 (2011) 1593–1599. https://doi.org/10.1039/c0jm02305a.

[14] H. Ota, Y. Sakata, Y. Otake, K. Shima, M. Ue, J. Yamaki, Structural and Functional Analysis of Surface Film on Li Anode in Vinylene Carbonate-Containing Electrolyte, J. Electrochem. Soc. 151 (2004) A1778. https://doi.org/10.1149/1.1798411.

[15] B. Zhu, Y. Jin, X. Hu, Q. Zheng, S. Zhang, Q. Wang, J. Zhu, Poly(dimethylsiloxane) Thin Film as a Stable Interfacial Layer for High-Performance Lithium-Metal Battery Anodes, Adv. Mater. 29 (2017) 2–7. https://doi.org/10.1002/adma.201603755.

[16] A.C. Kozen, C.F. Lin, A.J. Pearse, M.A. Schroeder, X. Han, L. Hu, S.B. Lee, G.W. Rubloff, M. Noked, Next-Generation Lithium Metal Anode Engineering via Atomic Layer Deposition, ACS Nano. 9 (2015) 5884–5892. https://doi.org/10.1021/acsnano.5b02166.

[17] Z. Wang, Z. Xu, X. Jin, J. Li, Q. Xu, Y. Chong, C. Ye, W. Li, D. Ye, Y. Lu, Y. Qiu, Dendrite-free and air-stable lithium metal batteries enabled by electroless plating with aluminum fluoride, J. Mater. Chem. A. 8 (2020) 9218–9227. https://doi.org/10.1039/d0ta02410d.

[18] D. Zhang, S. Wang, B. Li, Y. Gong, S. Yang, Horizontal Growth of Lithium on Parallelly Aligned MXene Layers towards Dendrite-Free Metallic Lithium Anodes, Adv. Mater. 31 (2019) 6–11. https://doi.org/10.1002/adma.201901820.

[19] G. He, Q. Li, Y. Shen, Y. Ding, Flexible Amalgam Film Enables Stable Lithium Metal Anodes with High Capacities, Angew. Chemie - Int. Ed. 58 (2019) 18466–18470. https://doi.org/10.1002/anie.201911800.

[20] X. Zhang, Q. Zhang, X.G. Wang, C. Wang, Y.N. Chen, Z. Xie, Z. Zhou, An Extremely Simple Method for Protecting Lithium Anodes in Li-O2 Batteries, Angew. Chemie - Int. Ed. 57 (2018) 12814–12818. https://doi.org/10.1002/anie.201807985.
[21] N.W. Li, Y. Shi, Y.X. Yin, X.X. Zeng, J.Y. Li, C.J. Li, L.J. Wan, R. Wen, Y.G. Guo, A Flexible Solid Electrolyte Interphase Layer for Long-Life Lithium Metal Anodes, Angew. Chemie - Int. Ed. 57 (2018) 1505–1509. https://doi.org/10.1002/anie.201710806.